Lyotropic Phase Behavior of Polybutadiene−Poly(ethylene oxide) Diblock Copolymers in Ionic Liquids

Peter M. Simone[†] and Timothy P. Lodge*[,†,‡]

Department of Chemistry and Department of Chemical Engineering & Materials Science, University of Minnesota, Minneapolis, Minnesota 55455

Received October 9, 2007; Revised Manuscript Received December 18, 2007

ABSTRACT: The lyotropic phase behavior of three poly(1,2-butadiene-*b*-ethylene oxide) diblock copolymers (PB−PEO) with different monomer volume fractions has been studied in two different ionic liquids, 1-ethyl-3-methylimidazolium bis(trifluoromethylsulfonyl)imide ([EMI][TFSI]) and 1-butyl-3-methylimidazolium hexafluorophosphate ([BMI][PF_6]), across the complete concentration range. The ordered microstructures present in the solutions were characterized via small-angle X-ray scattering (SAXS). The phase diagrams for the PB−PEO/ionic liquid solutions include regions corresponding to the classical copolymer microstructures: body-centered-cubic lattices of spheres, hexagonally ordered cylinders, and lamellae. Additionally, the phase diagrams also include wide regions of coexisting microstructures and regions apparently corresponding to a disordered network microstructure. The phase behavior of the PB−PEO copolymers in both ionic liquids was comparable to their previously reported aqueous solution behavior. The temperature dependence of the phase diagrams was very modest, indicative of a highly segregated system. The level of solvent selectivity was also investigated via cryogenic transmission electron microscopy (cryo-TEM) on dilute solutions. On the basis of the morphology of the dilute solution copolymer aggregate structures in the ionic liquid solvents, and on the structural length scales of the concentrated solutions, it was concluded that for PB−PEO [BMI][PF_6] behaves as a more selective solvent than [EMI][TFSI].

Introduction

The segregation of block copolymer molecules into microstructures consisting of regions rich in a single block type is a well-known and well-studied phenomenon.[1,2] The classical set of microstructures formed by simple A−B diblock copolymers includes spheres packed onto body-centered-cubic lattices (S), hexagonally packed cylinders (C), the bicontinuous gyroid (G), and lamellae (L). Essentially, block copolymer self-assembly is a result of the thermodynamic incompatibility between the chemically distinct blocks of the copolymer molecules. The stable microstructure for a particular block copolymer is determined by the copolymer composition (taken as the monomer volume fraction, f) and the degree of segregation between the blocks (χN), where χ is the Flory−Huggins interaction parameter and N is the total degree of polymerization.

Upon addition of a solvent to a block copolymer, a new, "effective" degree of segregation will be established, which will reflect the interactions between the blocks themselves and between the different blocks and the solvent. Thus, lyotropic phase transitions are often observed upon swelling a bulk copolymer with a solvent, since the effective degree of segregation may correspond to a different thermodynamically stable microstructure than that of the bulk sample. The lyotropic phase behavior for multiple block copolymer and solvent systems, both organic and aqueous, has been extensively studied.[3−17]

Recently, ionic liquids have emerged as a new class of solvents which consist entirely of ions. However, unlike more common ionic compounds, ionic liquids are composed of large, molecular ions that often possess some level of asymmetry and charge delocalization, which results in low lattice energies and melting points (often below room temperature).[18] In addition to melting points that are relatively low for ionic compounds, ionic liquids also possess many other appealing physical and chemical properties,[19,20] including extremely low vapor pressure, high thermal stability, and outstanding electrochemical behavior. In particular, electrochemical properties such as high ionic conductivity and wide electrochemical windows have led to research involving the use of ionic liquids as electrolyte materials for advanced devices such as lithium batteries,[21−27] fuel cells,[21,28−30] and dye-sensitized solar cells.[31−35] However, in many of these applications, a solid electrolyte would be easier to contain and more amenable to device production than a liquid. Thus, it is of interest to prepare solid, ionic liquid-based electrolytes by incorporating the ionic liquid into another material that will provide solid structure without greatly reducing the conductivity of the ions in the pure liquid.[36−61]

It could also be beneficial if the solid supporting material possessed an ordered nanostructure that could facilitate ionic conductivity in the solid ionic liquid electrolyte. Yoshio et al. and Ichikawa et al. have demonstrated this concept by incorporating an ionic liquid moiety into liquid crystalline molecules that self-assemble into well-defined nanostructures.[62,63] For some of the liquid crystalline molecules a subsequent photopolymerization step was used to stabilize the self-assembled microstructures. This same idea could be accomplished using the self-segregating behavior of block copolymers. If the ionic liquid used to swell the copolymer selectively interacts with one block over the other, then the majority of the liquid will be confined to that region of the copolymer microstructure. Ideally, then, the one-dimensional C phase (with ionic liquid selectively solvating the cylinder-forming block) would induce the most anisotropic character in ionic conductivity. However, the cylindrical nanostructure would require a subsequent step to induce macroscopic alignment of the randomly oriented microdomains. Thus, the G microstructure might be preferable. While the G morphology would induce greater tortuosity on ionic conductivity, the spontaneous formation of a continuous network

[†] Department of Chemistry.
[‡] Department of Chemical Engineering & Materials Science.

10.1021/ma702252v CCC: $40.75
Published on Web 02/09/2008

Table 1. Molecular Characteristics of PB−PEO Block Copolymers[a]

copolymers	M_{PB} (kg/mol)	M_{PEO} (kg/mol)	PDI[b]	f_{PEO}[c]
BO(9−6)	9.2	5.9	1.04	0.33
BO(9−4)	9.2	4.0	1.06	0.25
BO(9−3)	9.2	2.9	1.04	0.20

[a] Data reproduced from ref 67; PB block microstructure is 90% 1,2-addition. [b] Polydispersity index determined by size exclusion chromatography, calibrated with polystyrene standards. [c] PEO volume fraction determined by ^{1}H NMR.

throughout the entire macroscopic sample would eliminate the need for a separate microstructure alignment step. In addition, the block copolymer phase could provide mechanical robustness as compared to a simple liquid crystalline phase, without requiring a separate reaction following microstructure self-assembly.

To our knowledge there have been no systematic studies on the phase behavior of ionic liquid/copolymer systems. In this article we present the lyotropic phase behavior of poly(1,2-butadiene-*b*-ethylene oxide) diblock copolymers (PB−PEO) of differing composition, with the addition of 1-ethyl-3-methylimidazolium bis(trifluoromethylsulfonyl)imide ([EMI][TFSI]) and 1-butyl-3-methylimidazolium hexafluorophosphate ([BMI][PF_6]). [EMI][TFSI] was chosen because it has been widely used in many electrochemical applications and studies, due mainly to the low viscosities (i.e., high ionic diffusion coefficients) of most ionic liquids incorporating the [EMI] cation and the electrochemical stability of the [TFSI] anion.[64] [BMI][PF_6] was chosen because it is one of the most commonly studied ionic liquids, despite the higher viscosity and the less stable [PF_6] anion. Additionally, these two ionic liquids were chosen on the basis of the familiarity with their physical and chemical characteristics, and sample preparation techniques, from our previous studies.[59,61,65,66]

Experimental Section

Materials. The characteristics of the three PB−PEO block copolymers used in this study are shown in Table 1.

These copolymers were prepared previously via anionic polymerization,[67] and all possess the same butadiene block, with different length ethylene oxide blocks. [EMI][TFSI] was prepared via anion exchange between 1-ethyl-3-methylimidazolium bromide [EMI][Br] (Solvent Innovation) and lithium bis(trifluoromethylsulfonyl)imide ([Li][TFSI]) (IoLiTec) in water at 70 °C for 12 h. After the reaction the aqueous layer was removed, and the ionic liquid layer was repeatedly washed with distilled water. To further purify the ionic liquid, it was stirred over activated carbon (Sigma-Aldrich) for several hours. The final [EMI][TFSI] product was a clear, very faint yellow liquid. [BMI][PF_6] was purchased from Solvent Innovation and was a clear, colorless liquid. Both ionic liquids were dried under vacuum (≤50 mTorr) at 70 °C for at least 2 days and then stored in either a vacuum desiccator or glovebox under argon. The only extended exposure (several minutes) to atmospheric humidity was during sample preparation, after which samples were thoroughly dried. Thus, contamination by absorbed water is estimated to be minimal (<100 ppm). For [BMI][PF_6], Solvent Innovation specifies [Cl^-] < 100 ppm. [EMI][TFSI] was not tested for halide impurities; however, the slight yellow tint indicates a low level of impurity that could not be completely removed following synthesis. While trace impurities have been shown to significantly affect some physical properties of ionic liquids, it is unlikely that the ionic liquid solvation characteristics, which play the largest role in determining the copolymer morphology, would be influenced significantly.

Small-Angle X-ray Scattering. The PB−PEO/ionic liquid solutions for small-angle X-ray scattering (SAXS) experiments were prepared by combining the appropriate amounts of ionic liquid and copolymer, by weight, followed by dissolution in dichloromethane to form a dilute solution (ca. 5 wt % copolymer). The dilute solutions were stirred for several hours, and then the majority of the dichloromethane cosolvent was slowly evaporated under a dry nitrogen purge with stirring for 24 h. The samples were subsequently dried to constant weight under vacuum, with heating (ca. 30 mTorr, 65 °C). After drying, the PB−PEO/ionic liquid solutions were assembled into SAXS samples in the following manner. First, a hole was punched in an aluminum differential scanning calorimetry (DSC) pan, and a small circle of Kapton film (DuPont) was placed in the bottom of the pan to cover the hole. Next, a Teflon O-ring was placed in the DSC pan and filled with the PB−PEO/ionic liquid solution. Finally, a hole was punched in the DSC pan lid, and another circle of Kapton film was placed inside the lid to cover the hole. The DSC pan and lid were then crimped shut to seal the solution inside. After assembly, the SAXS samples were annealed under vacuum for 3 days at 80 °C. SAXS data were collected at the DuPont-Northwestern-Dow Collaborative Access Team (DND-CAT) beamline at the Advanced Photon Source, Argonne National Laboratory. Two-dimensional scattering patterns were recorded by a Mar CCD area detector and then azimuthally integrated to give one-dimensional scattering data as intensity (I) vs wave vector ($q = 4\pi \sin(\theta/2)/\lambda$), where θ is the scattering angle (calibrated with silver behenate) and λ is the X-ray wavelength. The sample-to-detector distances used were 869, 603, and 201 cm, and the X-ray wavelengths were 1.03, 0.827, and 1.03 Å, respectively. SAXS data were also collected on a home-built beamline at the University of Minnesota Characterization Facility. This beamline consisted of a Rigaku RU-200BVH rotating anode generating Cu Kα X-rays (λ = 1.54 Å), Franks mirror optics, a 230 cm flight tube, and a multiwire area detector (HI-STAR, Siemens Analytical X-ray Instruments). Representative one-dimensional scattering plots for the PB−PEO/ionic liquid solutions are shown in Figure 1.

Cryogenic Transmission Electron Microscopy. PB−PEO/ionic liquid solutions for cryogenic transmission electron microscopy (cryo-TEM) were prepared using the same method as described for the SAXS solutions above, except that the cosolvent was added in a 1:1 v/v dichloromethane to ionic liquid ratio. Cryo-TEM samples were prepared using microperforated copper TEM grids coated with a carbon-stabilized lacey Formvar support film (Ted Pella, Inc., Product No. 01883-F). The grids were suspended from tweezers in a temperature-controlled sample preparation chamber, and a small amount of copolymer solution was added to the grid using a micropipet. The majority of the solution was then blotted away using filter paper in order to obtain a thin solution layer (≤300 nm) that would span the holes of the lacey support film, yet still allow sufficient electron transmission during imaging. The [EMI][TFSI] samples were prepared at 25 °C, and the [BMI][TFSI] samples were prepared at 60 °C in order to reduce the ionic liquid viscosity to obtain sufficiently thin solution layers during blotting. Any shear stresses generated in the samples during blotting were allowed to relax for 60 s prior to vitrifying the solution by plunging the grid into liquid nitrogen. Once vitrified, the samples were kept under liquid nitrogen until being inserted into the microscope. The samples were examined using a JEOL 1210 TEM and a Gatan 626 cryogenic sample holder. The sample holder was cooled using liquid nitrogen and maintained a temperature of −175 °C while in the microscope. The microscope accelerating voltage was 120 kV, and images were recorded with a Gatan 724 multiscan CCD camera. The cryo-TEM images were analyzed using DigitalMicrograph software (version 3.3).

Results and Discussion

Phase Behavior for PB−PEO/[EMI][TFSI] Solutions. The phase behavior of the PB−PEO/[EMI][TFSI] system is shown in Figure 2a. The classical copolymer microstructures observed include a body-centered-cubic lattice of spherical PEO domains in a PB matrix (S_1^{bcc}) for the bulk BO(9−3) copolymer, hexagonally packed PEO cylinders (C_1), lamellae (L), and hexagonally packed PB cylinders (C_2). The subscript numbers

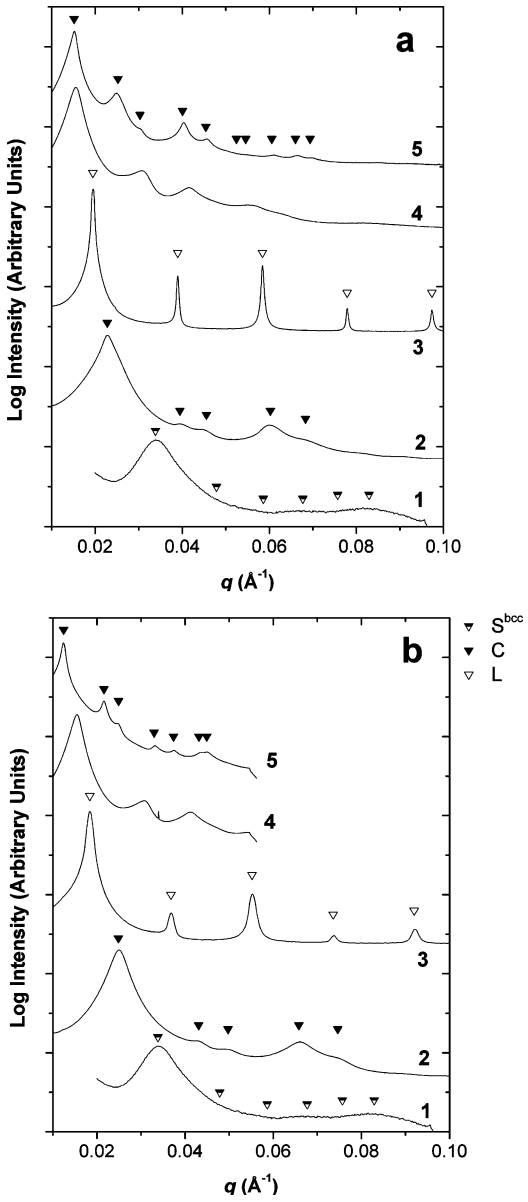

Figure 1. Representative 1D scattering plots for PB−PEO/ionic liquid solutions: (a**)** [EMI][TFSI]: 1, BO(9−3) bulk; 2, BO(9−3) 81 wt %; 3, BO(9−4) 60 wt %; 4, BO(9−6) 40 wt %; 5, BO(9−6) 30 wt %. (b**)** [BMI][PF_6]: 1, BO(9−3) bulk; 2, BO(9−4) 91 wt %; 3, BO(9−4) 60 wt %; 4, BO(9−6) 40 wt %; 5, BO(9−6) 17 wt %. Expected peak positions for S^{bcc}, C, and L are shown.

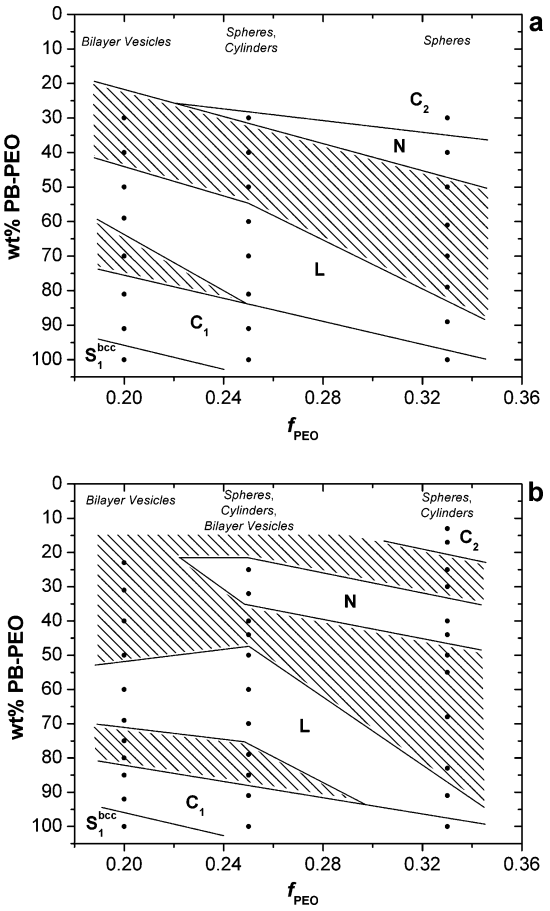

Figure 2. Lyotropic phase diagram for (a**)** PB−PEO/[EMI][TFSI] solutions and (b**)** PB−PEO/[BMI][PF_6] solutions at 25 °C. The *x*-axis corresponds to volume fraction of PEO in the bulk copolymers. The *y*-axis is the sample concentration in weight % copolymer. S is a cubic lattice of spheres, C is hexagonally packed cylinders, L is lamellae, and N is the disordered network of cylinders. Subscript 1 corresponds to normal microstructure (PB forming major microstructure domain), and subscript 2 corresponds to inverse microstructure (PEO and IL forming major microstructure domain). The filled areas correspond to regions of coexisting copolymer microstructures. Bilayer vesicles, cylinders, and spheres refer to the dilute solution copolymer aggregate structures determined via cryo-TEM.

associated with the microstructure labels indicate normal (PB blocks forming major microstructure domain) and inverse (PEO blocks and ionic liquid forming major microstructure domain) microstructures. Although SAXS cannot directly determine which copolymer block is preferentially solvated by [EMI]-[TFSI], PEO is readily soluble in many ionic liquids including those studied here, whereas PB is not. It is therefore clear that the ionic liquid is selective for the PEO blocks.

In addition to these classical block copolymer microstructures, the [EMI][TFSI] phase diagram includes regions that are not anticipated simply on the basis of a lyotropic progression of melt-phase block copolymer microstructures upon addition of solvent. First, regions of coexisting (L/C) microstructures occur in the phase diagram where the gyroid microstructure might be expected to appear. These regions are a result of the high degree of segregation between the blocks of the copolymers and the addition of solvent. The large interaction parameter χ between PB and PEO, and the increased effective χ upon addition of a very selective solvent, apparently makes the frustrated packing of the gyroid phase less thermodynamically favorable. The solvent adds another degree of freedom to the system, allowing the copolymers to rearrange in order to alleviate the packing frustration involved with the gyroid microstructure. The same phenomenon was reported by Hanley et al. for poly(styrene-*b*-isoprene) copolymers (PS−PI) in styrene-selective dialkyl phthalate solvents.[3,5] In these systems, the gyroid phase window yields to coexisting C and L microstructures upon increasing the solvent selectivity, either by decreasing temperature or by shortening the alkyl chains of the phthalate solvents.

Second, there exist phase regions characterized by scattering patterns containing broad peaks that cannot be referenced to the allowed reflections for any of the classic A−B diblock copolymer microstructures. We speculate that these regions of the PB−PEO/[EMI][TFSI] phase diagram are analogous to the disordered network microstructure observed by Jain et al. in PB−PEO/H_2O solutions on the basis of its location in the phase diagram and the similarity in the scattering profiles.[14] In the disordered network microstructure, the PB domain consists of branched, cylindrical struts, forming an irregular, three-dimensional network. The matrix is formed by the PEO blocks along with the ionic liquid. This region of the phase diagram is

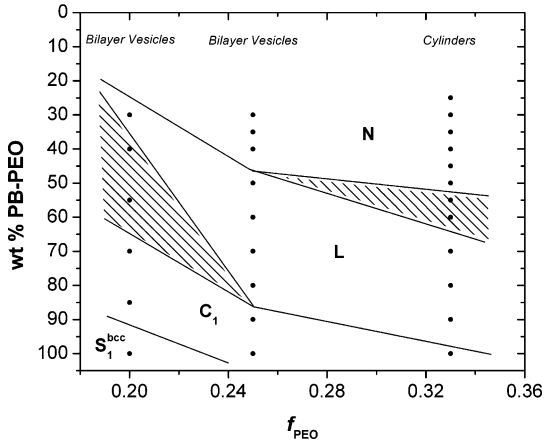

Figure 3. Lyotropic phase behavior for PB−PEO/H_2O solutions at 25 °C (adapted from ref 14). The *x*-axis corresponds to volume fraction of PEO in the bulk copolymers. The *y*-axis is the sample concentration in weight % copolymer. S is a cubic lattice of spheres, C is hexagonally packed cylinders, L is lamellae, and N is the disordered network of cylinders. Subscript 1 corresponds to normal microstructure (PEO and H_2O forming minor microstructure domain). The filled areas correspond to regions of coexisting copolymer microstructures. Bilayer vesicles and cylinders refer to the dilute solution copolymer aggregate structures determined via cryo-TEM.

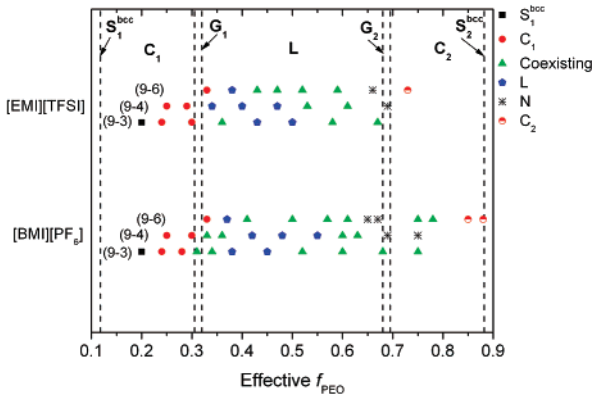

Figure 4. Experimentally observed microstructures for PB−PEO/ionic liquid solutions. Effective volume fraction of PEO calculated assuming the ionic liquid completely partitions into the PEO domains of the copolymer microstructure and using densities of 1.13, 0.87, 1.52, and 1.36 g/cm^3 for PEO, PB, [EMI][TFSI], and [BMI][PF_6], respectively. Vertical lines represent theoretical phase boundaries determined by Cochran et al.[70] There are no units corresponding to the *y*-axis. The microstructures for the solutions are shifted vertically for clarity.

therefore labeled N in Figure 2a, and the BO(9−6) 40 wt % scattering plot in Figure 1a is representative of those observed for the disordered network microstructure.

Phase Behavior for PB−PEO/[BMI][PF_6] Solutions. [BMI][PF_6] has been shown previously to behave as a selective solvent for the PEO blocks of the copolymers.[66] The lyotropic phase behavior for the PB−PEO/[BMI][PF_6] solutions (Figure 2b) is similar to that observed with the [EMI][TFSI] solvent. The classical microstructure phases of S_1^{bcc}, C_1, L, and C_2 are observed along with regions of coexisting (C/L) microstructures and the disordered network phase. The scattering pattern for the BO(9−6)/[BMI][PF_6] 40 wt % solution in Figure 1b is representative of those obtained for the network phase in [BMI][PF_6]. With both ionic liquid solvents, the network phase occurs between a region of coexisting microstructures, and a region of C_2 microstructure, similar to the phase behavior seen for the PB−PEO/H_2O solutions in Figure 3 (reconstructed from ref 14).

One method for qualitatively explaining the phase behavior for a copolymer/solvent system is to consider "trajectories" across the melt phase diagram for the copolymer. By assuming that a selective solvent completely partitions into the compatible block microdomain, then the addition of solvent can be converted to an increase in the soluble block volume fraction. This assumption was first introduced by Sadron and Gallot in the early 1970s[68] and was considered in more detail by Hanley et al.[3,5,69] Figure 4 shows the experimentally observed block copolymer microstructures for the PB−PEO/ionic liquid solutions, plotted by their effective PEO volume fractions, where effective f_{PEO} = (vol_{PEO} + vol_{IL}/total solution vol).

The phase boundaries shown in Figure 4 correspond to the theoretical phase boundaries determined for a bulk A−B diblock copolymer by Cochran and co-workers.[70] The large degree of segregation between the PB and PEO blocks results in χN > 100 for the three copolymers, which is in the region of the theoretical phase map where the boundaries are essentially vertical lines. Qualitatively, the experimental copolymer microstructures agree fairly well with the phase regions predicted by the theoretical boundaries. Thus, a horizontal trajectory across the phase diagram, corresponding to an increase in f_{PEO} upon addition of ionic liquid, provides an estimate of the lyotropic phase behavior for the PB−PEO/ionic liquid solutions. It can be noted that since the ionic liquids behave as selective solvents, the estimated trajectories should also include a vertical component corresponding to an increase in effective χ upon addition of the ionic liquid. However, since the χN of the PB−PEO copolymers places them in a region of the theoretical phase map where there is essentially no curvature of the phase boundaries, the vertical trajectory components are ignored. Figure 4 again illustrates that the regions of microstructure coexistence and network microstructure occur where the gyroid microstructure would be expected.

Ionic Liquid Solvent Selectivity. Dilute solution micellar aggregates formed by the PB−PEO copolymers in these ionic liquids suggest that [BMI][PF_6] behaves as a more selective solvent than [EMI][TFSI]. Figures 5 and 6 show cryo-TEM images of the aggregates formed by the three PB−PEO copolymers dissolved in [EMI][TFSI] and [BMI][PF_6], respectively, at a copolymer concentration of 1.0 wt %.

In the images, the densely packed PB blocks of the copolymers form the cores of micelles and the interior of bilayer sheets (forming vesicles), which can be seen as the lighter contrast structures in the dark vitrified solvent film. For the PB−PEO/[EMI][TFSI] solutions there is a progression from spherical micelles for BO(9−6), to larger spherical micelles with some short cylindrical micelles for BO(9−4), to bilayer vesicles for BO(9−3). For the PB−PEO/[BMI][PF_6] solutions, BO(9−6) forms spherical and short cylindrical micelles, BO(9−4) forms spherical and long cylindrical micelles and bilayer vesicles, and BO(9−3) forms bilayer vesicles and large structures that appear to be multiple vesicles fused together. The dominant factor in determining the morphology of dilute solution block copolymer aggregates is the core/corona interfacial tension. Increasing the selectivity of the solvent (i.e., increasing interfacial tension) will drive the aggregates toward morphologies with lower interfacial curvature. Thus, the formation of aggregates for a given copolymer with lower interfacial curvature in [BMI][PF_6] than in [EMI][TFSI] indicates that [BMI][PF_6] acts as the more selective solvent. Comparing the dilute solution aggregate behavior for the PB−PEO copolymers in ionic liquids to that observed by Jain et al. for aqueous PB−PEO solutions (Figure 3)[71] suggests that water acts as an even more selective solvent than either ionic liquid.

Additional supporting evidence for the higher selectivity of [BMI][PF_6] comes from comparing how the structural length

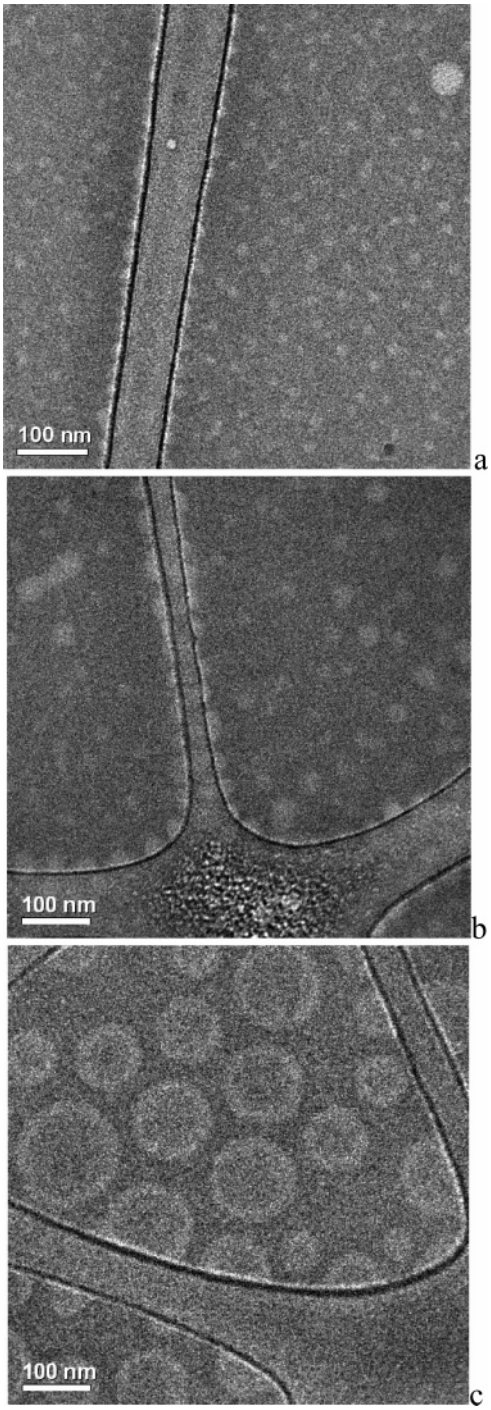

Figure 5. Cryo-TEM images of PB−PEO copolymers dissolved in [EMI][TFSI] at 1.0 wt %: (a**)** BO(9−6), (b**)** BO(9−4), and (c**)** BO-(9−3).

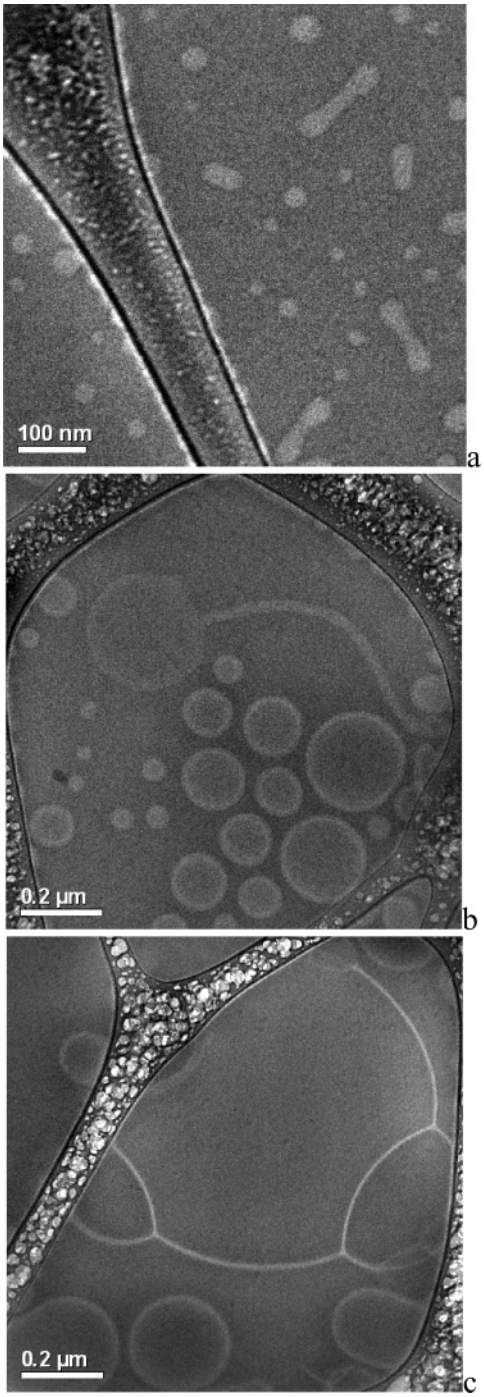

Figure 6. Cryo-TEM images of PB−PEO copolymers dissolved in [BMI][PF_6] at 1.0 wt %: (a**)** BO(9−6), (b**)** BO(9−4), and (c**)** BO-(9−3).

scale, taken as $d = 2\pi/q^*$ from the primary 100 scattering peak for the lamellar microstructure, differs based on ionic liquid. Figure 7 compares the lamellar structural length scale vs copolymer concentration for samples prepared with the two ionic liquids. Addition of a neutral solvent (i.e., one that solvates both copolymer blocks equally) will result in a decrease in structural length scale due to a general shielding of the unfavorable interactions between copolymer blocks, which allows increased lateral expansion of the blocks near the interface. Conversely, the addition of a selective solvent will cause an increase in structural length scale. This is due to a decrease in the interfacial area between block domains in order to reduce the unfavorable interactions between the solvent and the insoluble blocks, which results in increased chain stretching normal to the interface.

The overall result of larger domain spacing for [BMI][PF_6] samples indicates higher solvent selectivity of this ionic liquid. Additionally, the more negative slope for the fit of the [BMI]-[PF_6] domain spacing is another indicator of greater solvent selectivity. For comparison, theoretical self-consistent mean-field analysis of a lamellar forming system produced a power law exponent of −0.20 for a highly selective solvent (interaction parameter χ between solvent and insoluble block equal to 1).[5] In addition, these results compare favorably with the experimental results of Hanley et al. for a lamellar system consisting of a PS−PI diblock copolymer in diethyl phthalate (DEP) and dimethyl phthalate (DMP), which behave as selective and

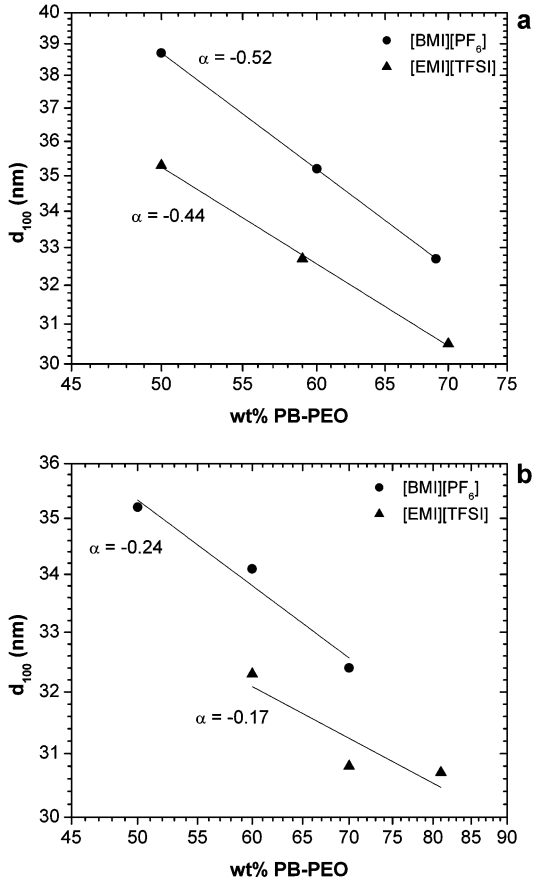

Figure 7. Dependence of lamellar domain spacing (d_{100}) on ionic liquid. Double-logarithmic plots, data fit with $d \sim (\text{concentration})^{\alpha}$: (a) BO(9−3) and (b) BO(9−4). Uncertainty in d_{100} is less than ±0.5 nm.

strongly selective PS solvents, respectively. In DEP $\alpha = -0.16$, and in DMP $\alpha = -0.61$.[5,72]

It is not surprising that the ionic liquids display less selective solvent behavior than water, since their molecular constituent ions allow them to participate in multiple solvent−solute interactions. It has been shown that various ionic liquids are capable of participating in both polar and nonpolar solvent−solute interactions.[73,74] If it is assumed that both [BMI][PF_6] and [EMI][TFSI] behave as equally good solvents for PEO, then it could also be assumed that [BMI][PF_6] should behave as a less selective solvent based on the increased possibility of dispersion interactions between the PB blocks and the butyl groups of the [BMI] cations, as compared to the ethyl group of the [EMI] cations. This hypothesis is supported by the results of Favre et al., who found that the solubility of 1-hexene in an ionic liquid with a constant anion increased along with the alkyl chain length of the 1-alkyl-3-methylimidazolium cation.[75] However, since [EMI][TFSI] displays less selective solvent behavior, this suggests that the solvent−solute interactions between the ionic liquid and the PB blocks are dependent upon the anion identity as well as the cation. Indeed, Favre et al. also observed greater 1-hexene solubility with the [TFSI] anion than with the [PF_6] anion in combination with [BMI].[75] This could be a result of the higher degree of charge delocalization present in the [TFSI] anion, which would result in a more favorable environment for the nonpolar PB blocks.

Conclusions

Using SAXS, the lyotropic phase behavior of PB−PEO diblock copolymers in ionic liquids has been investigated, and classical block copolymer microstructures, similar to those seen in systems with more common molecular solvents, have been observed. In addition to well-defined copolymer microstructures, evidence for the formation of a disordered cylindrical network microstructure, similar to that seen for the same PB−PEO block copolymers in water, was also observed. Cryo-TEM images of the dilute solution PB−PEO aggregate structures, and the structural length scales obtained from SAXS for the more concentrated solutions, show that [BMI][PF_6] behaves as a more selective solvent than [EMI][TFSI]. These results represent an important step in laying the foundation for a rational design of block copolymer ionic liquid composite materials, for diverse applications.

Acknowledgment. The authors thank Dr. Sumeet Jain for generously providing the PB−PEO copolymers used in this study. This work was supported by the National Science Foundation, through award DMR-0406656. Use of the Advanced Photon Source was supported by the U.S. Department of Energy, Office of Science, Office of Basic Energy Sciences, under Contract DE-AC02-06CH11357. Parts of this work were carried out in the University of Minnesota I.T. Characterization Facility, which receives partial support from NSF through the NNIN program and through the UMN MRSEC (DMR-0212302).

References and Notes

(1) Hamley, I. W. *The Physics of Block Copolymers*; Oxford University Press: Oxford, 1998.
(2) Bates, F. S.; Fredrickson, G. H. *Phys. Today* **1999**, *52*, 32−38.
(3) Lodge, T. P.; Pudil, B.; Hanley, K. J. *Macromolecules* **2002**, *35*, 4707−4717.
(4) Lai, C.; Russel, W. B.; Register, R. A. *Macromolecules* **2002**, *35*, 841−849.
(5) Hanley, K. J.; Lodge, T. P.; Huang, C.-I. *Macromolecules* **2000**, *33*, 5918−5931.
(6) Shibayama, M.; Hashimoto, T.; Hasegawa, H.; Kawai, H. *Macromolecules* **1983**, *16*, 1427−1433.
(7) Hamley, I. W.; Fairclough, J. P. A.; Ryan, A. J.; Ryu, C. Y.; Lodge, T. P.; Gleeson, A. J.; Pedersen, J. S. *Macromolecules* **1998**, *31*, 1188−1196.
(8) Pople, J. A.; Hamley, I. W.; Fairclough, J. P. A.; Ryan, A. J.; Komanschek, B. U.; Gleeson, A. J.; Yu, G. E.; Booth, C. *Macromolecules* **1997**, *30*, 5721−5728.
(9) Mortensen, K.; Brown, W.; Joergensen, E. *Macromolecules* **1994**, *27*, 5654−5666.
(10) Svensson, M.; Alexandridis, P.; Linse, P. *Macromolecules* **1999**, *32*, 637−645.
(11) Mortensen, K. *J. Phys.: Condens. Matter* **1996**, *8*, A103−A124.
(12) Almgren, M.; Brown, W.; Hvidt, S. *Colloid Polym. Sci.* **1995**, *273*, 2−15.
(13) Wanka, G.; Hoffmann, H.; Ulbricht, W. *Macromolecules* **1994**, *27*, 4145−4149.
(14) Jain, S.; Gong, X.; Scriven, L. E.; Bates, F. S. *Phys. Rev. Lett.* **2006**, *96*, 138304/138301−138304/138304.
(15) Foerster, S.; Berton, B.; Hentze, H. P.; Kraemer, E.; Antonietti, M.; Lindner, P. *Macromolecules* **2001**, *34*, 4610−4623.
(16) Hajduk, D. A.; Kossuth, M. B.; Hillmyer, M. A.; Bates, F. S. *J. Phys. Chem. B* **1998**, *102*, 4269−4276.
(17) Shibayama, M.; Hashimoto, T.; Kawai, H. *Macromolecules* **1983**, *16*, 16−28.
(18) Krossing, I.; Slattery, J. M.; Daguenet, C.; Dyson, P. J.; Oleinikova, A.; Weingaertner, H. *J. Am. Chem. Soc.* **2006**, *128*, 13427−13434.
(19) Wasserscheid, P., Welton, T., Eds. *Ionic Liquids in Synthesis*; Wiley-VCH: Weinheim, 2003.
(20) Forsyth, S. A.; Pringle, J. M.; MacFarlane, D. R. *Aust. J. Chem.* **2004**, *57*, 113−119.
(21) Fernicola, A.; Scrosati, B.; Ohno, H. *Ionics* **2006**, *12*, 95−102.
(22) Seki, S.; Kobayashi, Y.; Miyashiro, H.; Ohno, Y.; Mita, Y.; Usami, A.; Terada, N.; Watanabe, M. *Electrochem. Solid-State Lett.* **2005**, *8*, A577−A578.
(23) Seki, S.; Kobayashi, Y.; Miyashiro, H.; Ohno, Y.; Usami, A.; Mita, Y.; Kihira, N.; Watanabe, M.; Terada, N. *J. Phys. Chem. B* **2006**, *110*, 10228−10230.

(24) Garcia, B.; Lavallee, S.; Perron, G.; Michot, C.; Armand, M. *Electrochim. Acta* **2004**, *49*, 4583−4588.
(25) Hayashi, K.; Nemoto, Y.; Akuto, K.; Sakurai, Y. *J. Power Sources* **2005**, *146*, 689−692.
(26) Matsumoto, H.; Sakaebe, H.; Tatsumi, K.; Kikuta, M.; Ishiko, E.; Kono, M. *J. Power Sources* **2006**, *160*, 1308−1313.
(27) Sakaebe, H.; Matsumoto, H.; Tatsumi, K. *J. Power Sources* **2005**, *146*, 693−697.
(28) Belieres, J.-P.; Gervasio, D.; Angell, C. A. *Chem. Commun. (Cambridge, U.K.)* **2006**, 4799−4801.
(29) Nakamoto, H.; Watanabe, M. *Chem. Commun. (Cambridge, U.K.)* **2007**, 2539−2541.
(30) Susan, M. A. B. H.; Noda, A.; Mitsushima, S.; Watanabe, M. *Chem. Commun. (Cambridge, U.K.)* **2003**, 938−939.
(31) Wang, P.; Zakeeruddin, S. M.; Humphry-Baker, R.; Graetzel, M. *Chem. Mater.* **2004**, *16*, 2694−2696.
(32) Yamanaka, N.; Kawano, R.; Kubo, W.; Masaki, N.; Kitamura, T.; Wada, Y.; Watanabe, M.; Yanagida, S. *J. Phys. Chem. B* **2007**, *111*, 4763−4769.
(33) Gorlov, M.; Pettersson, H.; Hagfeldt, A.; Kloo, L. *Inorg. Chem.* **2007**, *46*, 3566−3575.
(34) Mazille, F.; Fei, Z.; Kuang, D.; Zhao, D.; Zakeeruddin, S. M.; Graetzel, M.; Dyson, P. J. *Inorg. Chem.* **2006**, *45*, 1585−1590.
(35) Fei, Z.; Kuang, D.; Zhao, D.; Klein, C.; Ang, W. H.; Zakeeruddin, S. M.; Graetzel, M.; Dyson, P. J. *Inorg. Chem.* **2006**, *45*, 10407−10409.
(36) Susan, M. A. B. H.; Kaneko, T.; Noda, A.; Watanabe, M. *J. Am. Chem. Soc.* **2005**, *127*, 4976−4983.
(37) Singh, B.; Sekhon, S. S. *Chem. Phys. Lett.* **2005**, *414*, 34−39.
(38) Tigelaar, D. M.; Waldecker, J. R.; Peplowski, K. M.; Kinder, J. D. *Polymer* **2006**, *47*, 4269−4275.
(39) Marwanta, E.; Mizumo, T.; Nakamura, N.; Ohno, H. *Polymer* **2005**, *46*, 3795−3800.
(40) Tiyapiboonchaiya, C.; Pringle, J. M.; MacFarlane, D. R.; Forsyth, M.; Sun, J. *Macromol. Chem. Phys.* **2003**, *204*, 2147−2154.
(41) Tiyapiboonchaiya, C.; MacFarlane, D. R.; Sun, J.; Forsyth, M. *Macromol. Chem. Phys.* **2002**, *203*, 1906−1911.
(42) Shin, J.-H.; Henderson, W. A.; Passerini, S. *J. Electrochem. Soc.* **2005**, *152*, A978−A983.
(43) Nakagawa, H.; Izuchi, S.; Kuwana, K.; Nukuda, T.; Aihara, Y. *J. Electrochem. Soc.* **2003**, *150*, A695−A700.
(44) Fuller, J.; Breda, A. C.; Carlin, R. T. *J. Electrochem. Soc.* **1997**, *144*, L67−L70.
(45) Li, Z.; Liu, Y.; Liu, H.; He, P.; Zhang, Q.; Li, J. *Solid State Ionics* **2006**, *177*, 1281−1286.
(46) Lewandowski, A.; Swiderska, A. *Solid State Ionics* **2004**, *169*, 21−24.
(47) Lewandowski, A.; Swiderska, A. *Solid State Ionics* **2003**, *161*, 243−249.
(48) Noda, A.; Watanabe, M. *Electrochim. Acta* **2000**, *45*, 1265−1270.
(49) Ohno, H.; Yoshizawa, M.; Ogihara, W. *Electrochim. Acta* **2003**, *48*, 2079−2083.
(50) Reiter, J.; Vondrak, J.; Michalek, J.; Micka, Z. *Electrochim. Acta* **2006**, *52*, 1398−1408.
(51) Kim, K.-S.; Park, S.-Y.; Yeon, S.-H.; Lee, H. *Electrochim. Acta* **2005**, *50*, 5673−5678.
(52) Shobukawa, H.; Tokuda, H.; Susan, M. A. B. H.; Watanabe, M. *Electrochim. Acta* **2005**, *50*, 3872−3877.
(53) Tigelaar, D. M.; Meador, M. A. B.; Bennett, W. R. *Macromolecules* **2007**, *40*, 4159−4164.
(54) Hanabusa, K.; Fukui, H.; Suzuki, M.; Shirai, H. *Langmuir* **2005**, *21*, 10383−10390.
(55) Bansal, D.; Cassel, F.; Croce, F.; Hendrickson, M.; Plichta, E.; Salomon, M. *J. Phys. Chem. B* **2005**, *109*, 4492−4496.
(56) Yeon, S.-H.; Kim, K.-S.; Choi, S.; Cha, J.-H.; Lee, H. *J. Phys. Chem. B* **2005**, *109*, 17928−17935.
(57) Singh, B.; Sekhon, S. S. *J. Phys. Chem. B* **2005**, *109*, 16539−16543.
(58) Seki, S.; Susan, M. A. B. H.; Kaneko, T.; Tokuda, H.; Noda, A.; Watanabe, M. *J. Phys. Chem. B* **2005**, *109*, 3886−3892.
(59) He, Y.; Boswell, P. G.; Buehlmann, P.; Lodge, T. P. *J. Phys. Chem. B* **2007**, *111*, 4645−4652.
(60) Kim, K.-S.; Park, S.-Y.; Choi, S.; Lee, H. *J. Power Sources* **2006**, *155*, 385−390.
(61) He, Y.; Lodge, T. P. *Chem. Commun. (Cambridge, U.K.)* **2007**, 2732−2734.
(62) Yoshio, M.; Kagata, T.; Hoshino, K.; Mukai, T.; Ohno, H.; Kato, T. *J. Am. Chem. Soc.* **2006**, *128*, 5570−5577.
(63) Ichikawa, T.; Yoshio, M.; Hamasaki, A.; Mukai, T.; Ohno, H.; Kato, T. *J. Am. Chem. Soc.* **2007**, *129*, 10662−10663.
(64) Galinski, M.; Lewandowski, A.; Stepniak, I. *Electrochim. Acta* **2006**, *51*, 5567−5580.
(65) Simone, P. M.; Lodge, T. P. *Macromol. Chem. Phys.* **2007**, *208*, 339−348.
(66) He, Y.; Li, Z.; Simone, P.; Lodge, T. P. *J. Am. Chem. Soc.* **2006**, *128*, 2745−2750.
(67) Jain, S.; Bates, F. S. *Macromolecules* **2004**, *37*, 1511−1523.
(68) Sadron, C.; Gallot, B. *Makromol. Chem.* **1973**, *164*, 301−332.
(69) Hanley, K. J.; Lodge, T. P. *J. Polym. Sci., Part B: Polym. Phys.* **1998**, *36*, 3101−3113.
(70) Cochran, E. W.; Garcia-Cervera, C. J.; Fredrickson, G. H. *Macromolecules* **2006**, *39*, 2449−2451.
(71) Jain, S.; Bates, F. S. *Science (Washington, D.C.)* **2003**, *300*, 460−464.
(72) Hanley, K. J. Block Copolymers: Phase Behavior in Neutral and Selective Solvents. Ph.D. Thesis, University of Minnesota, 2001.
(73) Armstrong, D. W.; He, L.; Liu, Y.-S. *Anal. Chem.* **1999**, *71*, 3873−3876.
(74) Anderson, J. L.; Ding, J.; Welton, T.; Armstrong, D. W. *J. Am. Chem. Soc.* **2002**, *124*, 14247−14254.
(75) Favre, F.; Olivier-Bourbigou, H.; Commereuc, D.; Saussine, L. *Chem. Commun. (Cambridge, U.K.)* **2001**, 1360−1361.

MA702252V